Preventive motor training but not progenitor grafting ameliorates cerebellar ataxia and deregulated autophagy in tambaleante mice

Preventive motor training but not progenitor grafting ameliorates cerebellar ataxia and deregulated autophagy in *tambaleante* mice

Elisa Fucà[1,2], Michela Guglielmotto[2], Enrica Boda[1,2], Ferdinando Rossi†, Ketty Leto[2*] and Annalisa Buffo [1,2*]

1. Department of Neuroscience Rita Levi-Montalcini, University of Turin, Italy

2. Neuroscience Institute Cavalieri Ottolenghi, Regione Gonzole 10043 Orbassano Turin, Italy

† Deceased 24 January 2014

*Co-last authors

Corresponding author

Elisa Fucà, Neuroscience Institute Cavalieri Ottolenghi Regione Gonzole 10043 Orbassano Turin, Italy

Tel 00 39 011 6706631

Email: elisa.fuca@unito.it

Authors' contribution

EF and KL performed grafts; EF performed motor training, behavioral, immunohistochemical analyses and stereological counts; MG and EB performed molecular biology and biochemical experiments; EF, FR, KL and AB conceived experiments, EF, KL and AB interpreted data and wrote the manuscript; all the authors reviewed and approved the final manuscript.

Highlights

- Preventive grafts of Purkinje cells survive despite ongoing host neurodegeneration
- Preventive cell transplantation does not ameliorate the progression of ataxic symptoms
- Preventive motor training improves ataxic symptoms
- Preventive motor training delays mutant PC loss and attenuates deregulated autophagy

Abbreviations

CB: calbindin

CN: cerebellar nuclei

PC: Purkinje cell

PNN: perineuronal net

tbl: tambaleante mutation

WT: wild type

Abstract

Treatment options for degenerative cerebellar ataxias are currently very limited. A large fraction of such disorders is represented by hereditary cerebellar ataxias, whose familiar transmission facilitates an early diagnosis and may possibly allow to start *preventive* treatments before the onset of the neurodegeneration and appearance of first symptoms. In spite of the heterogeneous aetiology, histological alterations of ataxias often include the primary degeneration of the cerebellar cortex caused by Purkinje cells (PCs) loss. Thus, approaches aimed at replacing or preserving PCs could represent promising ways of disease management. In the present study, we compared the efficacy of two different *preventive* strategies, namely cell replacement and motor training. We used *tambaleante (tbl)* mice as a model for progressive ataxia caused by selective loss of PCs and evaluated the effectiveness of the preventive transplantation of healthy PCs into early postnatal *tbl* cerebella, in terms of PC replacement and functional preservation. On the other hand, we investigated the effects of motor training on PC survival, cerebellar circuitry and their behavioural correlates. Our results demonstrate that, despite a good survival rate and integration of grafted PCs, the adopted grafting protocol could not alleviate the ataxic symptoms in *tbl* mice. Conversely, preventive motor training increases PCs survival with a moderate positive impact on the motor phenotype.

Keywords: neurotransplantation – Purkinje neurons - mouse - neurodegeneration -neuroprotection

1. Introduction

Cerebellar ataxias are a heterogeneous group of neurological disorders characterized by lack of motor coordination and imbalance associated with other typical clinical signs such as tremors, muscular hypotonia, oculomotor and speech impairment (Klockgether, 2007). To date, there are no effective cures for ataxias and the few pharmacological therapies tested persistence so far have revealed poor efficacy (Marmolino and Manto, 2010; IIg et al. 2014). Since Purkinje cell (PC) loss is the common and cardinal feature of these disorders (Sugawara et al., 2007), therapeutic strategies aimed at replacing and/or preserving these cells may represent promising options. However, approaches based on neurotransplantation at the symptomatic stages of the disease have been challenged by the low receptiveness for full integration of grafted cells of the mature nervous tissue (Carletti et al., 2002 and 2008; Carletti and Rossi, 2005). The integration of PC progenitors into host cerebellar cortex has been achievable only when progenitors have been grafted into very immature cerebella (Carletti et al., 2008). Thus, the window of opportunity for utilisation of grafting as a therapeutic approach precedes the common onset of the signs or symptoms of the pathology. Given this rationale, *preventive* neurotransplantation could be considered as an effective replacement therapy in the large fraction of hereditary cerebellar ataxias, wherein familiar transmission facilitates an early genetic diagnosis.

Among the non-invasive treatment options, motor exercise has been demonstrated to trigger neuroprotective mechanisms (Van Kummer and Cohen, 2015) and alleviate ataxic symptoms in both preclinical and clinical studies (Uhlendorf et al., 2011; Synofzik and Ilg 2014). However, the extent of this amelioration, as well as its endurance, is profoundly affected by factors such as the disease severity and areas of neurodegeneration, and becomes more limited with the progression of the pathology (Rabe et al., 2009; Miyai, 2012 a and b). Motor training at early and asymptomatic stages, when significant neurodegeneration and functional deterioration are absent, might exert more efficacious and lasting effects on the onset and progression of neurodegeneration, as well on the promotion of plasticity changes supportive for motor functions, thereby affecting the course of the disease. Therefore, the present study attempts to understand and compare the therapeutic effects of cell replacement or motor training as *preventive* approaches for cerebellar ataxia in homozygous *Tambaleante* (*tbl*) mice (Wassef et al., 1987).

Tbl mice exhibit a severe ataxic phenotype starting from two months of age, associated with abundant loss of PCs. The first sporadic manifestations of PC loss can be detected as early as at one

month of age (Mashimo, 2009). The subsequent massive degeneration of PCs has been attributed to the alteration of the HERC1 E3 ubiquitin ligase, which leads to overactive autophagic processes (Mashimo et al., 2009). PC degeneration in *tbl* mice occurs later compared to the other well-known spontaneous cerebellar mutation models, namely, the purkinje cell degeneration and lurcher mice (Mullen et al., 1976; Phillips, 1960). Thus, *tbl* mice represent an ideal opportunity to study preventive approaches in a timeline where PC degeneration has not yet begun. The uniqueness of this approach is its ability to showcase the effects of any adopted strategy specifically on the onset of the disease. Additionally, although signs of autophagy occur in extracerebellar neurons (Ruiz et al., 2016), consequential neurodegenerative processes only occur in PCs in *tbl* mice (Mashimo et al., 2009; Ruiz et al., 2016). This allows the investigation of the effects of preventive therapies on degenerative processes of a well-defined neuronal target.

In this study, we examined the effects of cell transplantation in postnatal *tbl* mice, when healthy PC progenitors are able to fully develop and integrate into host cerebellum. Next, we executed a protocol of preventive motor training daily to juvenile *tbl* mice until the day of sacrifice. We investigated the impact of such approaches on ataxic symptoms and neuronal degeneration. Our results demonstrate that, in spite of good survival and integration into host cerebellar cortex, grafted PCs do not alleviate the ataxic phenotype of *tbl* mice. In contrast, motor training attenuates ataxic symptoms and promotes PC survival with preservation of cerebellar circuitries and mitigation of autophagy deregulation.

2. Material and Methods

2.1. Animals and surgical procedures

Tambaleante heterozygous (+/–) mice were bred to produce wild-type (WT) and homozygous null littermates. Genomic DNA of transgenic mice was extracted from tail snips using standard protocols and examined by PCR-based genotyping using primers for WT and null alleles (Mashimo et al., 2009). Day of vaginal plug detection was defined as embryonic day 0 (E0), and the day of birth was considered as postnatal day 0 (P0). Pups were anesthetized by hypothermia.

Donor cells were isolated from the cerebellar primordium of E11 β-actin–GFP mice and grafted into the cerebellum of WT or mutant P1 littermates, as described (Jankovski et al., 1996; Carletti et al., 2002). The posterior surface of the cerebellum was exposed by removing a small fragment of the occipital bone. Two μl of the single-cell suspension (final concentration $5x10^4$ cells/μl),

obtained by mechanical dissociation was pressure-injected through a glass capillary into the parenchyma of cerebellar hemispheres in the attempt to increase the possibility for deep nuclei re-innervation from the grafted PCs. The wound was sutured, and the animal was returned to its cage. The recipient animals were sacrificed at 2 months post-transplantation.

All procedures on experimental animals were in accordance with the European Communities Council Directive (2010/ 63/EU), the National Institutes of Health guidelines, and the Italian Law for Care and Use of Experimental Animals (DL26/14) and were approved by the Italian Ministry of Health and the Bioethical Committee of the University of Turin.

2.2. Training procedures

Starting from P17, a group of *tbl* mice and their WT littermates underwent a protocol of motor training 5 days/week until the day of sacrifice (postnatal day 60). Motor training consisted of motor exercise (3' of climbing activity on cage and 20' of running wheel) and 6 crossing of a wooden beam bar with a rectangular section (1 cm x 1,5 cm), 1 m in length, placed 80 cm above a foam carpet.

2.3. Behavioural Assays

Rotarod test. The accelerated rotarod test was used to assess motor coordination and function (rotarod apparatus: Ugo Basile; five flanges divide the five 5.7 cm lanes, enabling five mice to be simultaneously on test, the cylinder diameter was 3.5 cm). Testing was performed once for month for mice of each group. Animals were put on the rotarod until the latency to fall off reached the total time of 300 s, with constant acceleration of 5.5 and maximum speed of 60 rpm. We performed three trials per day with 3-5 min intervals, on three consecutive days; the averages of the three sessions were considered. During pauses between trials, mice were allowed to rest in their home cages (adapted from Mashimo et al., 2009).

Beam walking test. Beam walking test was used to assess balance capabilities. Testing was performed once for month for mice of each group. The apparatus consisted of a motionless wooden beam with a rectangular section (1 cm x 3 cm), 1 m in length, placed 80 cm above a foam carpet. At the onset of the single trial, each animal was placed at the middle of the beam, its body axis being perpendicular to the beam long axis. We recorded the time spent to complete each cross and the number of slips made during the passages to the wooden bar, for a final number of 5 crossings to the bar. Then, for each animal, the walking speed and the frequency of slips were calculated; after 5

consecutive unsuccessful attempts to stay on the bar, the test was considered failed (adapted from Hilber and Caston, 2001). At two months of age, all *tbl* mice failed the test. After training number of slips and crossing time was calculated only for mice that completed the test.

2.4. Histological procedures

Under deep general anaesthesia, mice were transcardially perfused with 250 ml of 4% paraformaldehyde in 0.12 M phosphate buffer (pH 7.2-7.4). The brains were immediately dissected, postfixed overnight at 4°C and transferred to 30% sucrose in 0.12 M phosphate buffer. The cerebella were then embedded and frozen over dry ice in OCT (Tissue-Tek), sectioned in the parasagittal plane at 30 μm using a cryostat, and collected in PBS. Immunofluorescent staining of wild-type and mutant sections was performed in parallel to minimize inter-experiment variability. Primary antibodies were dissolved in PBS, with 1.5% normal serum and 0.25% Triton X-100, and incubated overnight at 4°C with: anti-calbindin (CB, 1:1500, Swant) to label PCs; anti-green fluorescent protein (GFP, 1:700, Invitrogen) and anti-GFP (1:700, Aves Labs) to enhance the GFP fluorescent signal of transplant-derived cells; anti-SMI32 (1:500, Sternberger) to label neurons in cerebellar nuclei (CN); anti-vesicular transporter for glutamate 1 - Vglut1 (1:1000, Synaptic System), anti-vesicular transporter for glutamate 2 - Vglut2 (1:1500, Synaptic System). For perineuronal nets (PNNs) visualization, sections were transferred to a solution containing biotinylated Wisteria floribunda agglutinin (WFA, 1:200, Sigma TM) for 2 h at room temperature and then in streptavidin-Alexa fluor 633. The sections were exposed or 1 hour at room temperature to secondary species-specific antibodies conjugated with Alexa Fluor 488, Alexa Fluor 555, or Alexa Fluor 647 (1:500; Invitrogen) or Cy3 (1:500; Jackson ImmunoResearch) or biotinylated secondary antibodies followed by streptavidin- Texas Red conjugate (1:200; Invitrogen). 4‟,6‟-diamidino-2-phenylindole (DAPI, Fluka) was used to counterstain cell nuclei. Finally, the sections were mounted in Mowiol (Calbiochem).

2.5. Tissue extracts and molecular analyses

Cerebella were manually dissected and divided in two hemicerebella by a sagittal cut along the vermis midline. For each individual, one hemicerebellum was used to quantify proteins while the other was employed to assess transcript levels. Total protein extracts were obtained from a 10% (w/v) homogenate of mouse cerebellar halves in RIPA buffer containing 0.5% Nonidet P-40, 0.5% sodiumdeoxycholate, 0.1% SDS, 10 mmol/l EDTA, and 1 mM DTT, 0.5 mM PMSF, 5 μg/ml aprotinin, and 2.5 μg/ml leupeptin. After 40 min of incubation in ice homogenates were cleared by

centrifugation at 15,000 g at 4 °C for 20 min. Supernatants were removed and stored. Protein content was determined using the Bradford assay. Protein extracts were stored at −80 °C until use. Twenty μg of samples were loaded.

We used polyclonal anti-microtubule-associated protein 1A/1B-light chain 3 LC3 (LC3, 1:800; Sigma-Aldrich, L8918) polyclonal anti- p62/sequestosome 1 (SQSTM1, 1:2000; Sigma-Aldrich, P0067) and monoclonal anti-β-actin (1:1000; Sigma-Aldrich) for this analysis. Total extracts were separated on 9.3% sodium dodecyl sulfate-polyacrylamide gels (Sigma-Aldrich, 01708), using a mini-PROTEAN II electrophoresis cell (Bio-Rad, 165-3301). Proteins were transferred onto nitrocellulose membranes (GE-Healthcare, RPN203D). Nonspecific binding was blocked with 50g/l nonfat dry milk in 50 mM TRIS-HCl, pH 7.4, containing 200 mM NaCl and 0.5 mM Tween-20. The blots were incubated with different primary antibody, followed by incubation with peroxidase-conjugated anti-mouse (Bio-Rad, 170-6516) or anti-rabbit (Bio-Rad, 170-6515) immunoglobulins in Tris-buffered saline Tween [150 mM sodium chloride solution (Sigma-Aldrich, S6546) 10 mM TRIS-HCl pH 7.4 (Sigma Aldrich, T5941) 0.05% Tween 20 (Sigma-Aldrich, P1379)] containing 20g/l nonfat dry milk. Reactions were developed with an enhanced chemiluminescence system according to the manufacturer's protocol (Bio-Rad, 170-5061). To compare the density of protein bands of interest and test for significant differences between samples in Western blotting experiments, blots were scanned and quantified using Quantity One Analysis Software (Bio-Rad). Data from band quantification were normalized on levels of β-Actin bands.

For quantitative Real time PCR (RT q-PCR) analyses, total RNA was isolated with the TRIzol Reagent (Invitrogen Life Technologies Inc., Grand Island, NY, USA), in accordance with the manufacturer's instructions. 0.5 microgram of total RNA was reverse-transcribed to complementary DNA (cDNA) using the High-Capacity cDNA Archive Kit (Life Technologies), according to the manufacturer's instructions. Quantitative real-time PCR was carried out using the StepOne Plus Real Time PCR System and TaqMan Gene Expression Assays (probes: Bdnf, cod. Mm04230607_s1; b-Act, cod. Mm00607939_s1). Data extracted from each run were analysed with a relative quantification approach as in Livak and Schmittgen (2001).

2.6. Morphometric analyses

2.6.1. Morphometry of PCs and their terminals

PC density was measured as described in Carulli et al. (2002) on anti-CB immunolabeled sections. The size of PC somata was assessed by drawing their outline and measuring the corresponding areas in about 40 PC cell bodies/animal by means of the Neurolucida software (MicroBrightField) connected to an E-800 Nikon microscope with a 40 × objective. PC terminals on CN projection neurons - identified by size and SMI32 expression (Leto et al., 2006) - were analysed for density along the postsynaptic somata and size by means of ImageJ software. Measurements were performed on single confocal optical sections (1-μm-thick), captured under a 63x objective (80–320 calbindin-positive terminals from at least 3 animals/experimental condition). All measurements were performed on CN neurons in which the nucleus was visible in the optical section. Changes in size after motor training in both WT and *tbl* animals were also evaluated by calculating the ratio between the measurements of button sizes in normal and training conditions in each strain.

2.6.2 Spine and VGlut1/2 terminal counts

In randomly selected PCs in lobule II, we analyzed the density of dendritic spines along the dendritic tree in confocal optical sections (1-μm-thick). Spine numbers were obtained by counting all spines along 100 randomly selected 5-μm segments including both proximal and distal dendritic domains of 10 different PCs (adapted from Magrassi et al., 2013). With a similar approach, we analyzed the number of $Vglut1^+$ terminals of parallel fibers contacting distal PC dendrites as well as that of $Vglut2^+$ terminals on the proximal shaft, where climbing afferents establish their contacts. Densities of $VGlut1/2^+$ terminals of lobule II were obtained by counting the number of terminals along 50 randomly selected 5-μm dendritic segments in 10 different PCs. These analyses were performed using ImageJ software.

2.6.3. Quantification of PNN number and density

The percentage of CN SMI32-positive projection neurons bearing a PNN was determined on double labeled sections with SMI32 antibodies and WFA or anti-Sema3A antibodies (3 sections/mouse, 3 mice/experimental condition). The analysis of WFA staining intensity, performed on the medial nucleus, was adapted from Foscarin et al. (2011). Briefly, single 1 μm-focal plane confocal images were collected under a 63 × objective. On such images we measured the mean brightness intensity (range 0–255) of 25-30 PNNs/animal by using ImageJ. The background brightness, taken from a non-stained region of the cortical molecular layer, was subtracted from the brightness measurements. Each net was then assigned to one of three categories of staining intensity, ranging

from the lowest to the highest value of WFA intensity detected: weak = 0–33%, medium = 34–66%, strong = 67–100% of maximum staining intensity.

2.7. Image acquisition

Histological specimens were examined using an E-800 Nikon microscope connected to a color CCD camera and a Leica TCS SP5 confocal microscope. Confocal images were acquired at a resolution of 512x512 dpi and 100 Hz speed and each focal plane was 1-µm- thick. Laser intensity, gain and offset were maintained constant in each analysis. Quantitative and morphometric evaluations were made by blind observers using the software Image J (http://rsbweb.nih.gov/ij/index.html, Research Service Branch) - as described in Leto et al., 2011 - and Neurolucida (MicroBrightField), the latter connected to the E-800 Nikon microscope via a color CCD camera. Adobe Photoshop 6.0 (Adobe Systems) was used to adjust image contrast and assemble the final plates. Measurements were derived from at least three sections per animal. Three to six animals were analysed for each time point or experimental condition.

2.8. Statistical analyses

Data elaboration and statistical analyses were conducted by means of GraphPad software Prism version 7.0 (GraphPad software, San Diego). In all instances, *P<0.05 was considered as statistically significant, **P<0.01 very significant and *** P<0.001 extremely significant. Graphs and data are represented as means ± standard deviation unless specified. If data sets passed normality test and equal variance test, we performed Student's t-test or One/Two Way Anova followed by Bonferroni *post hoc* tests. Pearson's R was used for correlation analysis. When data did not satisfy the normality or equal variance tests, corresponding non-parametric statistics was used. To compare different percentages, we transformed the values in radiants according to the arcsin transformation. We used Chi-square test to compare the distribution of frequencies with respect to staining intensity categories. Details about statistical assessment can be found in Table 1.

3. Results

3.1. *Tbl* mice displayed ataxia-like symptoms and progressive PC degeneration

Homozygous *tbl* mice showed a severe ataxia-like phenotype including unstable gait, abnormal hind limb-clasping reflex and tremor (data not shown), as already described (Mashimo et al., 2009). These mice also performed significantly worse than their WT littermates in motor function tests like the rotarod test as early as at one month of age (Fig. 1A, Two Way Anova P <0.0001). At this time

point, further balance assessment on the wooden beam revealed significant impairment in the overall performance, with a significant higher number of slips observed in *tbl* mice (Fig. 1B; Student's t-test $P<0.05$). Additionally, the the time taken to complete the crossing on the beam bar was significantly higher in *tbl* mice (Fig. 1C; Student's t-test $P<0.05$). The performance of WT mice on motor function tests did not alter over time, while the *tbl* mice displayed dramatic and progressive worsening of performance in the motor function tests (Fig. 1A-C). This effect was especially prominent on the beam bar test, wherein the *tbl* mutant mice were unable to complete the task by two months of age, due to their inability to stay on the bar itself (Fig. 1B,C). Regarding the histological phenotype of *tbl* cerebella, only sporadic signs of PC loss could be observed at one month of age (Mashimo et al., 2009, data not shown). A prominent reduction (approximately 85%) in the linear density of PCs manifested only at two months (Fig. 2A, E; Student's t-test $P<0.0001$), which progressed to an almost total loss after the fourth month of age, as indicated by anti-CB immunostaining (Fig. 2B-D, F; One way Anova $P<0.05$). The PC degeneration followed a caudo-rostral gradient, with PCs located in caudal lobules such as lobule VI or X being less preserved than those of rostral lobule II (Fig. 2G-J; One Way Anova $P<0.05$). However, PCs surviving at two months displayed clear regressive changes, as shown by a smaller body size with respect to their WT counterparts (Fig. 2K-M; Student's t-test $P<0.05$).

3.2. Healthy wild type PCs integrate and mature in *tbl* cerebella but do not ameliorate motor deficit

Tbl mice represent a model of ataxia associated with progressive neurodegeneration of PCs in the absence of gross defects in other CNS areas (Mashimo et al., 2009, our observations, data not shown). It is therefore valid to hypothesize that the replacement of degenerated PCs with healthy counterparts through transplantation might alleviate motor impairment at least to a certain degree. Numerous studies have demonstrated that the immature cerebellum provides the ideal environment for the most effective integration of transplanted neurons. Hence, we tested the impact of preventive grafts of cerebellar progenitors transplanted in neonatal mutant mice. We injected a donor cell suspension obtained from the cerebellar anlage of β-actin–GFP transgenic mice at embryonic day 11 (E11) in the cerebellar parenchyma of the *tbl* recipient. We specifically selected this time point since most PC progenitor are generated around E11 and constitute a major proportion in this territory. The animals were analysed 2 months post transplantation. Transplanted cells in the host tissue were identified by the strong intrinsic fluorescence and could be found either scattered through the recipient tissue, or clustered with other donor cells.

To begin with, we assessed the degree of graft integration. Only distinguishable individual cells identified on the basis of distinctive morphological features as well as expression of specific markers (GFP and CB) were considered as donor-derived engrafted elements. Both WT (Fig. 3A-C) and *tbl* recipients (Fig. 3D-H) showed a similar degree of donor cell integration and differentiation. The largest amount of grafted PCs was found in the cerebellar hemispheres, as expected according to the site of injection, with about one third of the grafted cells integrated in the cerebellar vermis (not shown). Donor-derived PCs were distributed in numerous lobules including crus2, simple, lobules III, IV, V, VI. They displayed mature morphologies and were well integrated in the cerebellar architecture of the host. Cell bodies of grafted PCs aligned along the host PCL (Fig. 3A-B, D-F) or remained slightly ectopic in the molecular layer (Fig. 3B,G), as expected in this experimental approach (Carletti et al., 2008). A minor fraction of donor-derived PCs was ectopically located in the granule cell layer (GL) and white matter (WM) region (Fig. 3B). Donor PC axons also reached their natural targets in the CN (Fig. 3C, H). Numbers of ectopic PCs in the GL/WM and CN regions were also similar in both wild type and mutant recipients, representing the 10.9% of total donor-derived PCs in wild-type hosts (i.e. 62 out of 566 PCs, 3 mice, 1 series of sections out of a total of six for each cerebellum) and the 7.8% in mutants (ie 44 out of 559 PCs, 3 mice, 1 series of sections out of a total of six for each cerebellum). The phenotypic repertoire of cells composing the grafts was comparable both in WT and mutant hosts (Fig. 3I,J): E11 donor cells produced a prominent fraction of PCs immunolabeled by CB, and minor fractions of CN neurons, GABAergic interneurons and glial cells, as previously demonstrated (Leto et al., 2006; Carletti et al., 2008). Additionally, donor-derived PCs showed cell body sizes larger than those of the endogenous *tbl* counterparts and fully comparable to WT cells of the same age (Fig. 3K-M; One Way Anova $P<0.05$). Thus, they maintained a healthy phenotype despite exposure to the mutant environment. Immunolabelling with the antibody anti-Vglut2 revealed the presence of synaptic connectivity between grafted cells and recipient tissue (Fig. 3N). Since progenitor cells are known to release factors that may promote neuroprotection (Martino and Pluchino, 2006), we hypothesised that grafts could exert neuroprotective actions on degenerating PCs. However, the overall density of endogenous PCs in grafted mutants did not undergo significant changes upon transplantation (Fig. 3O). To better clarify this point, we also examined the linear density of endogenous PCs as a function of the density of grafted PCs in the corresponding lobules (see Supplementary Fig. 1A). However, no significant variations were found associated with increasing numbers of donor PCs (One way Anova). These data were further analysed by correlation analysis that showed a poor Pearson's coefficient ($R=0.22$, $P=0.34$). Thus, the density of integrated cells did not affect the

survival of endogenous PCs. In summary, grafted cerebellar progenitors survived and attained a good degree of integration but did not impact on the progression of neurodegeneration.

We then assessed whether the grafts ameliorated motor dysfunctions in *tbl* mice. At both one and two months of age grafted mutant mice showed compromised motor abilities in both the rotarod (Fig. 3P; Two way Anova $P<0.0001$) and beam tests (Fig. 4Q, R; Student's t test $P<0.05$). Unexpectedly, no improvements were detected in comparison with *tbl* mice without grafts, showing no impact of transplantation on motor deterioration. Thus, *preventive* PC grafts were not effective in decelerating endogenous PC degeneration or attenuating the impaired motor phenotype in *tbl* mutants.

3.3. Preventive motor training promotes PC survival and improves motor functions in *tbl* mice

In order to assess whether PC degeneration in *tbl* mice could be delayed by enhanced physical activity, we tested a protocol of motor training administered 5 days/week starting from P17, until the day of sacrifice at two months of age. Motor training included running wheel, climbing and balance exercises. We sacrificed the trained animals two months after birth. PC density in trained mutants revealed a significant 50% increase compared to their sedentary counterparts (Fig 4A, Student's t-test $P<0.05$). Nevertheless, *tbl* trained mice showed a pattern of PC degeneration similar to their untrained siblings with a relative preservation of anterior lobes compared to the posterior ones. A more detailed evaluation of PC densities in trained *tbl* animals in lobules II/IV/X revealed that, despite *tbl* trained mice showed a global trend to have higher numbers of endogenous PCs in all lobules, PC survival was significantly higher only in lobule II (Fig. 4 B-D, Two way Anova $P<0.05$), which is naturally the most preserved in *tbl* mice at 2 months of age. Such increase in PC density was accompanied by a full reversion of *tbl* cell body atrophy in the same lobule (Fig. 4E-G, Student's t-test $P<0.05$).

Importantly, these morphological changes were accompanied by a significant amelioration of the motor deficits of trained mutants. Trained *tbl* mice improved their performance on the rotarod test at one month of age (Fig 4H, Two-way Anova $P<0.0001$) and reached levels of WT sedentary animals. However, thereafter their performance deteriorated. However, their latency to fall remained slightly higher than their untrained siblings. Amelioration in balance abilities was also detected with the beam walking test: at one month of age, *tbl* trained mice displayed a performance resembling that of WT sedentary animals. Remarkably, at difference from their sedentary counterparts at two months of age 50% of the trained mutants were able to successfully complete

the beam walking test, despite their performance remained worse compared to WT mice (Fig 4I One way Anova $P<0.01$ and J One way Anova $P<0.01$). Thus, preventive motor training not only delayed the progression of PC degeneration, but also positively affected the motor phenotype of mutant mice.

3.4. Molecular mechanisms underlying protective effects of motor training

Based on evidence that motor training provides neuroprotection in neurodegenerative diseases – including ataxia (Spires et al., 2004; Rolland et al., 2008; Fryer et al., 2011; Lin et al., 2015) and that motor training promotes PC survival, we investigated whether neuroprotective mechanisms were induced in *tbl* mice after motor training. We investigated the levels of BDNF, a neurotrophin known to be enhanced by motor activity (Huang et al., 2014), to promote PC survival (Van Kummer and Cohen, 2015) and to be expressed by different cell types in the cerebellum including PCs, granule cells, glia and interneurons (Vazquez-Sanroman et al., 2013, Supplementary Fig. 1B). We found that levels of BDNF were significantly increased in response to motor training in both WT and *tbl* trained cerebella compared to those of sedentary mice in terms of both mRNA and protein amounts (Fig. 5A-C; One way Anova $P<0.05$ for WT and $P<0.01$ for *tbl*). Interestingly, BDNF has been shown to exert neuroprotective effects through modulation of the autophagic flux (Chen et al., 2013; Smith et al., 2014; Bak et al, 2015) which is involved in PC death in *tbl* mutants (Mashimo et al 2009, Dusart et al., 2006). Hence, we set out to monitor the effects of motor training on autophagy. We found that while LC3 - I and II - and Beclin 1, considered as markers for accumulation of autophagosomes, were increased in trained WT cerebella suggesting incremented autophagy (Fig. 5D, F, G One way Anova $P<0.0001$), they decreased in tissues of trained mutants (Fig. 5E, F, G; One way Anova $P<0.0001$), indicating an attenuation of induced autophagy. Such a divergent modulation, implying a potentiated autophagic flux in WT and a decreased one in *tbl* mice, was confirmed by consistent and significant changes in the protein levels of p62/SQSTM1 (Fig. 5H, I; One way Anova $P<0.01$ for WT and $P<0.001$ for *tbl*), which is a substrate of autophagy whose amount corresponds to active degradation mechanisms (Komatsu et al., 2007).

Taken together, these data suggest that BDNF upregulation and attenuation of the pathologic autophagic flux contribute to slower neurodegeneration following motor exercise. Interestingly, they show that the impact of motor training and BDNF upregulation diverges in WT and mutant mice, indicating that outcomes strongly depend on contextual tissue conditions.

3.5. Preventive motor training preserves connections in cerebellar circuits and PNN

Based on evidence that environmental stimulation modulates the density of synaptic contacts on PCs (Kim et al., 2002; Lee et al., 2007), we asked whether motor activity could influence afferents and efferents connections implicated in the deterioration of motor performances in mutant mice. To gain a degree of understanding into changes elicited by motor training, we focused on lobule II where PC survival was the maximum, and analysed excitatory inputs from parallel and climbing fibres to PCs as well as PC spine densities. Moreover, we examined the fastigial and interpositus CN, where PCs of the spinocerebellum including lobule II, project their terminals.

The parallel fibre inputs from granule cells on PC distal dendrites were analysed by means of anti-Vglut1 antibodies that specifically label these excitatory terminals in the adult cerebellum (Fremeau et al., 2001). In sedentary conditions, *tbl* mice displayed a reduction of up to 21% in the anti-Vglut1^{+} terminals compared to WT cells. After motor training, a significant 15% increment was observed (Fig 6A) in the parallel inputs of *tbl*, whereas, there was no change was detected in WT animals (Fig. 6A, Two way Anova $P<0.001$). We then examined the other excitatory input to PCs, provided by climbing fibre terminals of inferior olivary neurons. These afferents, impinging on PC proximal dendrites and recognized by anti-Vglut2 antibodies (Ichikawa et al., 2002), were reduced by about 50% compared to WT cells (Fig. 6D). Similar to what was found for parallel inputs, whilst motor exercise did not change the density of climbing fiber terminals in WT mice, it lead to a significant increase in mutant mice (20% increase, Fig. 6B-D Two way Anova $P<0.001$). Changes in terminal densities together with rescue of soma atrophy in mutants prompted us to assess whether exercise also impacted on PC spine density. We found that training induced about a 50% increased in the number spines in mutant PCs (Fig. 6E-G, Student's t test: $P=0.005$).

As formerly shown (Foscarin et al., 2011), enhanced physical activity induces significant changes in the innervation provided by PCs to Smi32^{+} excitatory projection neurons in the CN. After confirming that the *tbl* mutation does not alter size or number of these neurons (data not shown), we assessed if and how motor training affected number and size of PC synaptic terminals on CNs. Two months-old *tbl* mice exhibited larger (Fig. 6H, Two-way Anova $P<0.01$) but less numerous CB^{+} synaptic terminals compared to controls (Fig. 6I; Two-way Anova $P<0.001$; Supplementary Fig. 1C, D), as already found in other conditions of partial denervation (Carulli et al., 2013;). We found a trend for an increase in area and density of PC terminals after physical exercise in both WT and *tbl* populations (Fig. 6H, I). However, such differences reached statistical significance only in PC

terminal density of WT animals. Conversely, CB^+ terminal density was steady for all the groups of mutants, including grafted mice (Supplementary Fig. 1E).

Finally, we focused on PNNs which are components of extracellular matrix that enwrap the perikaryon of defined neuronal subtypes, including excitatory large projection neurons in the CN (Carulli et al., 2006). Their formation contributes to the closure of critical periods and their reduction has been associated with the induction of plasticity windows (Pizzorusso et al., 2002; Foscarin et al., 2011). In the cerebellum, PNNs around CN neurons are deposited by both PC and CN neurons during the first weeks of life in rodents (Carulli et al., 2006, 2007, 2011). Our analysis of PNN density at two months of age revealed that a smaller fraction of CN neurons in sedentary *tbl* mice possessed PNNs, compared to untrained WT mice (Fig. 6J, One way Anova $P<0.05$). This finding is in line with the degeneration of PCs that actively contribute to PNN deposition and maintenance around CN neurons (Foscarin et al., 2011; Carulli et al., 2013) After motor training, while WT animals displayed a significant reduction of PNNs density (Fig. 6J; Two-way Anova $P<0.05$), as expected for conditions that elicit functional plasticity (Foscarin 2011; Madinier et al., 2014). However, mutants showed a 20% increment in the frequency of the nets, though difference is not statistically significance. Additionally, the latter data were strengthened by analysis of the intensity of PNNs, where we found significant changes in the distribution of weak, medium and strong intensity nets only in mutant mice (Fig. 6K-M). After exercise, the proportions of net types were maintained in WT CN. Conversely, the frequency of nets classified as strong or medium increased to reach about 70% in mutants (Fig. 6K; Chi-square $P<0.05$), thereby matching the distribution of WT PNNs (Chi-square $P>0.05$).

Taken together, these data indicate that motor exercise impact on cerebellar circuitry by limiting alterations occurring in *tbl* mutants.

4. Discussion

In this study we examined the ability of cerebellar progenitor grafts performed early postnatally to sustain normal cerebellar functions and to promote survival of Purkinje neurons in the *tbl* model of cerebellar ataxia. In parallel, we investigated the effects of preventive motor training on the onset and progression of the disease. We found that while transplantation of healthy cerebellar progenitors did not produce significant effects either on endogenous PC density or on motor behaviour, motor exercise promoted PC survival, reduced alterations of cerebellar circuits, and improved both motor coordination and balance capabilities in mutant mice.

Transplantation of distinct types of neural progenitors or stem cells has been broadly tested for replacement of degenerated PCs and/or rescue of functional deficits in several ataxia mouse models (for review, see Cendelin, 2016). Functional benefits were obtained after bilateral transplantation of foetal cerebellar cell suspension directly into the CN of adult *pcd* (Triarhou et al., 1996) or SCA1 mice (Kaemmereer and Low, 1999), or the depth of vermis in Lurcher mice (Babuska et al., 2015). In our study, cerebellar precursor grafts performed at ages that allow proper integration of PCs, failed to produce significant effects on motor behavior. This occurred despite good survival and correct placement of donor cells, suggesting that their number and/or the type of newly formed connections were not adequate to vicariate the degenerating circuits in supporting cerebellar functions. In regard to the number of grafted cells, we cannot exclude that a higher amount of injected precursors could lead to motor improvement in *tbl* mutants. However, this study is within the range of amount of grafted cell, formerly shown to have a positive impact on motor functions (cfr Triarhou et al., 1996; Kaemmerer and Low, 1999; Babuska et al., 2015). This observation, together with results of former studies (Triarhou et al., 1996), suggests that a critical aspect linked to the lack of functional improvement in our transplantation approach may be an insufficient establishment of connections between grafted PCs and CNs. Also, grafted precursors did not impact significantly on the survival of endogenous mutant PCs, a beneficial effect generally promoted by transplantation of undifferentiated neural stem cells or mesenchymal stem cells (Li et al., 2006; Jones et al., 2010), and often associated with functional benefits (Kaemmerer and Low, 1999; Jones et al., 2010 and 2015; Babuska et al., 2015). In our approach, neuroprotective factors produced by undifferentiated precursors may have decreased soon after grafting due to precursor differentiation, therefore failing to effectively promote cell survival. Taken together, our results suggest that early progenitor grafts *per se* do not represent a preventive strategy effective to counteract emerging histological and functional deficits in cerebellar ataxia, at least with the described grafting protocol. The lack of beneficial functional effects upon grafting prevented the investigation of potential common mechanisms underlying the behavioral improvement instead found with the second tested strategy, that is, *preventive* motor training.

Motor exercise triggered a significant enhancement in both motor coordination and balance capabilities in mutant mice that, especially at earlier time points, performed remarkably better than their sedentary counterparts. Behavioral improvements induced by rehabilitation approaches are generally attributed to preservation and/or plastic modification of the affected circuits (Churchill et al., 2002; Kleim and Jones, 2008; Austin et al., 2014; Huang et al., 2014). The detected increase in

tbl PC survival, reduced atrophy and increased afferent contacts to *tbl* PCs, clearly show that physical exercise activated protective mechanisms in mutant mice. However, additional mechanisms such as a reduction of neuromuscolar junction alterations described in *tbl* mice (Bachiller et al., 2015) could also contribute to the detected functional benefits. A better preservation of cerebellar neurons is in line with the increased deposition of PNN in CN, and it is further strengthened by the incremented expression of BDNF in combination with reduction of deregulated autophagy. Yet, PNN and BDNF are also key regulators of neural plasticity (Gomez-Pinilla et al., 2002; Foscarin et al., 2011; Wang et al., 2015). PNNs are accumulation of extracellular matrix molecules deposited after birth that stabilise synapse and restrict neural plasticity (Foscarin et al., 2011; Sale et al., 2007). At mature stages, environmental stimulation including motor training fosters PNN attenuation, which allows plastic changes of connectivity, including compensatory remodelling (Sale et al., 2007; Foscarin et al., 2011; Carulli et al., 2013). Of note, PNN deposition around CN neurons occurs during the second week of life in rodents (Carulli 2007) and depends on the interplay between PCs and CN neurons (Blosa et al., 2016). The reduction in PNN numbers and partial loss of PC terminals in sedentary mutants well fits with the PNN attenuation found both in models of PC denervation (Foscarin et al., 2011; Carulli et al., 2013) and in developmental and adult models of reduced GABAergic activity (Harauzov et al., 2010; McRae et al., 2012; Blosa et al., 2016). On the contrary, increased PNN staining after physical exercise in *tbl* mice is consistent with a better survival and functioning of mutant PCs, that led to increased net deposition. In WT trained mice, PNN reduction together with changes in PC terminal number and size, are instead fully in line with plastic modifications formerly shown after environmental stimulation (Foscarin et al., 2011; Carulli et al. 2013). On the whole, these data indicate that motor training mainly impacted on survival mechanisms in *tbl* mice while in WT animals promoted plastic changes. However, we cannot exclude that plastic modifications in extra-cerebellar motor centers of *tbl* mice may play a role in the detected amelioration of motor behavior (Jones et al., 1999; Tamakoshi et al., 2014).

Interestingly, BDNF, which we found upregulated in both trained mutant and WT animals, constitutes a key signal for both neuroprotection and neural plasticity (Chen et al., 2013; Smith et al., 2014; Bak et al., 2015). BDNF overexpression in mutants confirms former studies, where motor training-induced protection from neurodegeneration was associated with elevated levels of BDNF and its receptor TrkB in the cerebellum (Klintosova et al., 2004; Van Kummer and Cohen, 2015). Data in WT mice are instead in line with evidence showing that physical activity-dependent

increase in BDNF levels promotes brain plasticity (Farmer et al., 2004; Vaynman et al., 2004; Hopkins et al., 2011; Vivar et al., 2013; Ieraci et al., 2015). Thus, in our models, overexpression of BDNF likely participates in the promotion of either protection or plasticity, respectively in mutant or WT mice.

Consistent with divergent effects of motor training, we also show opposite changes in autophagy in WT and *tbl* mice. Autophagy is a mechanism essential for maintaining cellular homeostasis in both physiological functioning and pathology, where excessive or insufficient autophagic flux can promote cell death (Puyal et al., 2012; Zhao et al., 2015). While motor exercise triggers increased autophagy in WT mice, it dampens the deregulated flux in *tbl* mutants. Increased autophagy associated with brain plasticity was also reported in healthy rats after motor exercise-induced adaptation; here, autophagy upregulation has been put in correlation with high-energy demanding from mitochondria (Marques-Aleixo et al., 2015). Yet, both increased and decreased autophagy promoted cell survival in numerous models of neuronal damage (Puyal et al., 2012). Intriguingly, BDNF has been implicated in bidirectional modulation of the autophagic flux through pathways converging on mTOR (Smith et al., 2014; Bak et al, 2015). On the other side, in a model of cellular stress, elevated BDNF has been shown to promote neuron survival by suppressing autophagy *via* the activation of mTOR (Smith et al., 2014). This latter mechanism could attenuate autophagy in *tbl* mice, where decreased mTOR activity takes part in PC death (Mashimo et al., 2009). Taken together, these findings show that motor training-induced BDNF upregulation associates with opposite changes in the autophagic flux, in turn stimulating cell survival or plastic changes. Opposite outputs downstream of training and BDNF overexpression may depend on the fine-tuning of common molecular cascades responding to intrinsic homeostatic factors. In case of *tbl* mice, enhanced BDNF levels could cause adaptive stress-response, thus increasing resistance to excessive autophagy. However, the molecular mechanisms driving the switch toward divergent responses remain to be clarified.

In summary, *preventive* motor training delays the deterioration of motor functions by attenuating the progression of PC neurodegeneration. These results therefore enforce the use of preventive motor exercise in inherited ataxia to promote a delay in the progression of the disease, and indicate that this approach could be a promising step toward the amelioration of patients' quality of life.

Conflict of interest

The authors declare no conflict of interest.

Acknowledgments

We thank Ishira Nanavaty and Tommaso Iozzo for assistance with behavioral tests and Daniela Carulli for the support to analysis of PNNs. This work was supported by Research Fund for the Promotion of Basic Research Grant RBFR10A01S (K.L.) and by the University of Turin.

Figure legends

Fig.1 Motor impairment of *tbl* mice. We compared motor performances of *tbl* mice with wild-type littermates. Motor coordination of mutant mice was assessed by rotarod test until 2 months of life: latency to fall was significantly lower compared to controls already at 1 month of age (A; Two way Anova $P<0.0001$). The wooden beam test further revealed balance impairment at one month of age (B, C; Student's t test $P<0.05$). At two months of age, mutant mice were not able to walk on the wooden bar therefore we did not score the test. Data are represented as means ± standard error. N=6/group.

Fig.2 Pattern of PC degeneration in *tbl* mice. The analysis of linear density of PCs along the entire Purkinje Cell Layer in sections of cerebellar vermis of mutant mice showed that, at two months of age, cell degeneration affecting *tbl* cerebella causes a prominent loss of PCs, especially in lobule X - arrowhead - with relative preservation of PCs in lobule II - arrow (A, E; Student's t test $P<0.0001$) and a further significant decrease in the subsequent months (F, One way Anova $P<0.05$). After 4 months of age, degeneration accounts for about 95% of PCs present in WT animals (B-F). PC degeneration in two-months-old *tbl* mice proceeds according to a posterior-anterior gradient, as revealed by analysis of cerebellar vermis (A, G-J; One way Anova $P<0.05$), with a relative sparing of the most anterior lobes in the earliest phases of the disease. At two months of age, *tbl* PCs exhibit smaller body size compared to wild-type littermates (K-M; Student's t test $P<0.05$). N=3/group. Scale bars: A-I 100 μm; K-L 10 μm.

Fig.3 Preventive transplantation of healthy PCs in *tbl* mice allows correct cell integration but does not improve motor behavior. Transplanted PC progenitors are able to engraft both WT (A-

C) and *tbl* cerebella (D-H), displaying successful and correct integration into host PCL (A, B, D, E, F), in spite of occasional misplacing (B, G, H). Some axons of grafted PCs reached the CN regions (C, H). After transplantation, cerebellar progenitors mainly gave rise to PCs in both WT and mutant environments (I, J). Grafted PCs maintained a normal body size (K), larger than their endogenous counterparts (L, M), thus suggesting that the mutant environment did not affect their functions. The presence of Vglut-2^+ terminals on grafted PCs (N) further indicates functional integration. The analysis of the density of PCs along the entire Purkinje Cell Layer in sections of both vermis and hemispheres revealed that transplantation did not significantly increase the number of endogenous PCs in *tbl* mice (O). Evaluation of motor function did not detect any improvement in *tbl* grafted mice either in motor coordination (P, Two way Anova $P<0.0001$. Data are represented as means ± standard error) or in balance capabilities (Q, R. Student's t test $P<0.05$. Data are represented as means ± standard error). N=5/group. Scale bars: A, B, H, I 100 μm; C, D, L 50μm; E-F 40 μm; G 20μm; N 5μm.

Fig.4 Preventive motor training promotes PC survival and motor function improvement in *tbl* mice. *Tbl* mice exposed to preventive motor training exhibited a significant higher PC density, as calculated along the entire Purkinje Cell Layer in both vermis and hemispheres compared to their sedentary counterparts (A-D; Student's t test $P<0.05$). Trained mutant mice displayed an increased in PC density in all cerebellar lobules, but the increment in the number of PCs was significantly higher than mutant controls only in lobule II (B, Two way Anova $P<0.05$). Here, motor training also promoted an increase of *tbl* PC body size (E-G, Student's t test $P<0.05$). Trained *tbl* mice performed better than their sedentary counterparts at both rotarod at two months of age (H, Two way Anova: $P<0.001$. Data are represented as means ± standard error) and beam walking test (I, One way Anova $P=0.01$; J One way Anova $P<0.01$). Data are represented as means ± standard error). N=6/group. Scale bars: C, D 100 μm, D, H, I 5μm.

Fig.5 Neuroprotection and modulation of autophagic process after motor training. After motor training an increase in mRNA levels for BDNF was detected in both WT and *tbl* mice (A-C). Western blot analysis confirmed the significant upregulation of BDNF protein levels in both WT and *tbl* groups (B, C; One way Anova $P<0.05$ for WT and $P<0.01$ for *tbl*). WT animals showed an increase in Beclin1 and LC3 autophagy-related proteins in the cerebellum after motor training (D, F, G; One way Anova $P<0.0001$). On the contrary, in trained *tbl* cerebella a significant reduction of these proteins compared to their sedentary counterparts was detected (E, F, G; One way Anova $P<0.0001$). A significant reduction of p62 levels occurred in WT trained animals while it was

accumulated in mutant mice after training (H, I; One way Anova P<0.01 for WT and P<0.0001 for *tbl*). N=5 for WT mice; N=4 for *tbl* mice.

Fig.6 Motor training promotes the preservation of cerebellar connections and PNN on CN neurons. After motor training, *tbl* mice showed a significant increase in the number of Vglut1$^+$ terminals (A; Two way Anova P<0.001). A similar effect could be observed in the number of Vglut2$^+$ terminals (B-D; Two way Anova P<0.001). The number of spines in trained mutant mice was also increased compared to their sedentary counterparts (E-G; Student's t-test P<0.001). In trained cerebella there was the tendency in having larger CB$^+$ terminals on CN neurons display an increase in size (H). However, this trend was statistically significant only for WT animals (H; Two way Anova P<0.05). The same trend for a increment was detectable in the density of CB$^+$ terminals; however, the number of CB$^+$ terminals in tbl mice remained significantly lower to WT in both conditions (I; Two way Anova P<0.001). Analysis of the frequency of PNN around excitatory CN projection neurons revealed that *tbl* sedentary mice possess a reduced number of PNNs compared to WT; yet, preventive motor training significantly decreased PNN density in WT group with essentially no changes in *tbl* cerebella (J, Two way Anova P<0.05). However, whereas the proportions of PNN with distinct intensities did not vary in WT trained cerebella, trained *tbl* mice exhibited a significant expansion of PNNs with medium or strong intensities (K-M; Chi-square P<0.05). N=3/group. Scale bars: B, C, F, G 5µm; F^i and G^i 2µm; L, M 10µm.

Supplementary Fig.1: (A) The linear density of endogenous PCs does not vary as a function of the density of grafted PCs in the corresponding lobules (One Way Anova). Grafted PC densities were classified according to three categories: 1-15 PCs/lobule/slice, 16-30 PCs/lobule/slice and more than 31 cells/lobule/slice. (B) BDNF staining confirmed its expression in PCs, granule cells and some interneurons of the molecular layer in WT animals. (C, D) Two-months old *tbl* mice exhibit larger CB$^+$ terminals compared to WT animals; some CB$^+$ terminals are indicated by the arrows. (E) The comparison of CB$^+$ terminal densities revealed no significant differences in the three groups of mutant mice. For grafted mice, both endogenous and grafted PC terminals were considered in this quantification.

References

Austin MW, et al., 2014. *Aerobic exercise effects on neuroprotection and brain repair following stroke: a systematic review and perspective*. Neurosci Res; 87:8–15.

Babuska V. et al., 2015. *Transplantation of Embryonic Cerebellar Grafts Improves Gait Parameters in Ataxic Lurcher Mice*. Cerebellum. Dec;14(6):632-41. doi: 10.1007/s12311-015-0656-x.

Bachiller S., et al., 2015. *The HERC1 E3 Ubiquitin Ligase is essential for normal development and for neurotransmission at the mouse neuromuscular junction*. Cell Mol Life Sci. Aug;72(15):2961-71.

Bak DH, et al., 2015. *High ω3-polyunsaturated fatty acids in fat-1 mice prevent streptozotocin-induced Purkinje cell degeneration through BDNF-mediated autophagy*. Sci Rep. Oct 27;5:15465.

Blosa M., et al., 2016. *Reorganization of Synaptic Connections and Perineuronal Nets in the Deep Cerebellar Nuclei of Purkinje Cell Degeneration Mutant Mice*. Neural Plast.2016:2828536.

Carletti, B. et al., 2002. *Specification of cerebellar progenitors following heterotopic/heterochronic transplantation to the embryonic CNS in vivo and in vitro*. J. Neurosci. 22, 7132–7146.

Carletti B. et al., 2008. *Time constraints and positional cues in the developing cerebellum regulate Purkinje cell placement in the cortical architecture.* Developmental Biology 317, 147–160.

Carletti B., Rossi F., 2005. *Selective rather than inductive mechanisms favour specific replacement of Purkinje cells by embryonic cerebellar cells transplanted to the cerebellum of adult Purkinje cell degeneration (pcd) mutant mice*. European Journal of Neuroscience, Vol. 22, pp. 1001–1012.

Carulli D., et al., 2002. *Regenerative and survival capabilities of Purkinje cells overexpressing c-Jun.* Eur J Neurosci. Jul;16(1):105-18.

Carulli D., et al., 2006. *Composition of perineuronal nets in the adult rat cerebellum and the cellular origin of their components*. J Comp Neurol. Feb 1;494(4):559-77.

Carulli D., et al., 2007. *Upregulation of aggrecan, link protein 1, and hyaluronan synthases during formation of perineuronal nets in the rat cerebellum*. J Comp Neurol. 2007 Mar 1;501(1):83-94.

Carulli D., et al., 2011. *Activity-dependent plasticity and gene expression modifications in the adult CNS*. Front Mol Neurosci. 2011 Nov 28;4:50.

Carulli D., et al., 2013 *Modulation of semaphorin3A in perineuronal nets during structural plasticity in the adult cerebellum*. Mol Cell Neurosci. 2013 Nov;57:10-22.

Cendelin J., 2016. *Experimental neurotransplantation treatment for hereditary cerebellar ataxias*. Cerebellum Ataxias. Apr 4;3:7.

Chen A., et al., 2013 *The neuroprotective roles of BDNF in hypoxic ischemic brain injury*. Biomed Rep. Mar;1(2):167-176.

Churchill JD, et al., 2002 *Exercise, experience and the aging brain*. Neurobiol Aging 23: 941–955.

Dusart I., et al., 2006. *Purkinje cell death: differences between developmental cell death and neurodegenerative death in mutant mice.* Cerebellum.;5(2):163-73.

Farmer J., et al., 2004. *Effects of voluntary exercise on synaptic plasticity and gene expression in the dentate gyrus of adult male Sprague-Dawley rats in vivo*. Neuroscience. 2004;124(1):71-9.

Foscarin S., et al., 2011. *Experience-dependent plasticity and modulation of growth regulatory molecules at central synapses*. PLoS One. Jan 31;6(1):e16666.

Fremeau RT Jr, et al., 2001. *The expression of vesicular glutamate transporters defines two classes of excitatory synapse*. Neuron. Aug 2;31(2):247-60.

Fryer JD, et al., 2011. *Exercise and genetic rescue of SCA1 via the transcriptional repressor Capicua*. Science. Nov 4;334(6056):690-3.

Gómez-Pinilla F. et al., 2002. *Voluntary exercise induces a BDNF-mediated mechanism that promotes neuroplasticity*. J Neurophysiol. Nov;88(5):2187-95.

Harauzov A., et al., 2010. *Reducing intracortical inhibition in the adult visual cortex promotes ocular dominance plasticity*. J Neurosci. Jan 6;30(1):361-71.

Hilber P., Caston J., 2001. *Motor skills and motor learning in Lurcher mutant mice during ageing*. Neuroscience; 102(3):615–23.

Hopkins ME, et al., 2011. *Physical exercise during adolescence versus adulthood: differential effects on object recognition memory and brain-derived neurotrophic factor levels*. Neuroscience. Oct 27;194:84-94.

Huang T., et al., 2014. *The effects of physical activity and exercise on brain-derived neurotrophic factor in healthy humans: A review*. Scand J Med Sci Sports. Feb;24(1):1-10.

Ichikawa R., et al., 2002. *Distal extension of climbing fiber territory and multiple innervation caused by aberrant wiring to adjacent spiny branchlets in cerebellar Purkinje cells lacking glutamate receptor delta 2*. J Neurosci. Oct 1;22(19):8487-503.

Ieraci A. et al., 2015. *Physical exercise and acute restraint stress differentially modulate hippocampal brain-derived neurotrophic factor transcripts and epigenetic mechanisms in mice*. Hippocampus. Nov;25(11):1380-92.

Ilg W., et al., 2014. *Consensus Paper: Management of Degenerative Cerebellar Disorders*. Cerebellum 2014. 13:248–268.

Jankovski A., et al., 1996. *Neuronal precursors in the postnatal mouse cerebellum are fully committed cells: evidence from heterochronic transplantations*. Eur J Neurosci. Nov;8(11):2308-19.

Jones J., et al. 2010. *Mesenchymal stem cells rescue Purkinje cells and improve motor functions in a mouse model of cerebellar ataxia*. Neurobiol Dis. 2010 Nov;40(2):415-23.

Jones J., et al., 2015. *Mesenchymal stem cells improve motor functions and decrease neurodegeneration in ataxic mice.* Mol Ther. Jan;23(1):130-8.

Jones T., et al., 1999. *Motor skills training enhances lesion-induced structural plasticity in the motor cortex of adult rats*. J Neurosci. 15;19(22):10153-63.

Kaemmerer WF, Low WC, 1999. *Cerebellar allografts survive and transiently alleviate ataxia in a transgenic model of spinocerebellar ataxia Type-1*. Exp Neurol.;158:301–11.

Kim HT, et al., 2002. *Specific plasticity of parallel fiber/Purkinje cell spine synapses by motor skill learning*. Neuroreport 13:1607–1610.

Kleim JA, Jones TA, 2008. *Principles of experience-dependent neural plasticity: implications for rehabilitation after brain damage*. J Speech Lang Hear Res; 51:S225–S239.

Klintsova AY., et al., 2004. *Altered expression of BDNF and its high-affinity receptor TrkB in response to complex motor learning and moderate exercise*. Brain Res. 1028, 92–104.

Klockgether T., 2007. Ataxias. *Parkinsonism Relat Disord 13* (Suppl 3):S391–S394.

Komatsu M., et al., 2007. *Homeostatic levels of p62 control cytoplasmic inclusion body formation in autophagy-deficient mice*. Cell. Dec 14;131(6):1149-63.

Lee KJ, et al., 2007. *Morphological changes in dendritic spines of Purkinje cells associated with motor learning*. Neurobiol Learn Mem. Nov;88(4):445-50.

Leto K., et al., 2006. *Different types of cerebellar GABAergic interneurons originate from a common pool of multipotent progenitor cells*. J Neurosci. Nov 8;26(45):11682-94.

Leto K., et al., 2011. *Modulation of cell-cycle dynamics is required to regulate the number of cerebellar GABAergic interneurons and their rhythm of maturation*. Development.138(16):3463-72.

Li J., et al., 2006. *Neural stem cells rescue nervous purkinje neurons by restoring molecular homeostasis of tissue plasminogen activator and downstream targets*. J Neurosci. 2006 Jul 26;26(30):7839-48.

Lin TW, et al., 2015. *Running exercise delays neurodegeneration in amygdala and hippocampus of Alzheimer's disease (APP/PS1) transgenic mice*. Neurobiol Learn Mem. Feb;118:189-97.

Livak KJ, Schmittgen TD., 2001. *Analysis of relative gene expression data using real-time quantitative PCR and the 2(-delta delta CT) method*. Methods 25:402–408.

Marques-Aleixo I., et al., 2015. *Physical exercise prior and during treatment reduces sub-chronic doxorubicin-induced mitochondrial toxicity and oxidative stress.* Mitochondrion. Jan;20:22-33.

Madinier, A., et al., 2014. *Enriched Housing Enhances Recovery of Limb Placement Ability and Reduces Aggrecan-Containing Perineuronal Nets in the Rat Somatosensory Cortex after Experimental Stroke*. PLoS One. 2014 Mar 24;9(3):e93121.

Magrassi L., et al., 2013. *Lifespan of neurons is uncoupled from organismal lifespan*. Proc Natl Acad Sci U S A. 2013 Mar 12;110(11):4374-9.

Marmolino D., Manto M., 2010. *Past, present and future therapeutics for cerebellar ataxias* Curr Neuropharmacol. Mar;8(1):41-61.

Mashimo T., et al., 2009. *Progressive Purkinje cell degeneration in tambaleante mutant mice is a consequence of a missense mutation in HERC1 E3 ubiquitin ligase*. PLoS Genet. Dec;5(12):e1000784

Martino G., Pluchino S., 2006. *The therapeutic potential of neural stem cells*. Nat Rev Neurosci. May;7(5):395-406.

McRae PA, Porter BE, 2012. *The perineuronal net component of the extracellular matrix in plasticity and epilepsy*. Neurochem Int. Dec;61(7):963-72.

Miyai I., 2012a. C*hallenge of Neurorehabilitation for Cerebellar Degenerative Diseases*. Cerebellum 11:436–437.

Miyai I., et al., 2012b. *Cerebellar Ataxia Rehabilitation Trial in Degenerative Cerebellar Diseases*. Neurorehabilitation and Neural Repair 26(5) 515–522.

Mullen RJ, et al., 1976. *Purkinje cell degeneration, a new neurological mutation in the mouse.* Proc Nat Acad Sci U S A 73:208–212.

Phillips, RJS, 1960. '*Lurcher', a new gene in linkage group XI of the house mouse*. J. Genet. 57, 35–42.

Pizzorusso T., et al., 2002. *Reactivation of ocular dominance plasticity in the adult visual cortex.* Science. Nov 8;298(5596):1248-51.

Puyal J., et al., 2012. *Neuronal autophagy as a mediator of life and death: contrasting roles in chronic neurodegenerative and acute neural disorders*. Neuroscientist. 2012 Jun;18(3):224-36.

Rabe K., et al. 2009. *Adaptation to visuomotor rotation and force field perturbation is correlated to different brain areas in patients with cerebellar degeneration*. J Neurophysiol.101:1961–71.

Rolland Y,. et al., 2008. *Physical activity and Alzheimer's disease: from prevention to therapeutic perspectives*. J Am Med Dir Assoc. Jul;9(6):390-405.

Ruiz R., et al., 2016. *HERC 1 Ubiquitin Ligase Mutation Affects Neocortical, CA3 Hippocampal and Spinal Cord Projection Neurons: An Ultrastructural Study*. Front Neuroanat. Apr 18;10:42.

Sale A., et al., 2014. *Environment and brain plasticity: towards an endogenous pharmacotherapy*. Physiol Rev. Jan;94(1):189-234.

Smith ED, et al., 2014. *Rapamycin and interleukin-1β impair brain-derived neurotrophic factor-dependent neuron survival by modulating autophagy*. J Biol Chem. Jul 25;289(30):20615-29.

~~Sotelo C., Alvarado-Mallart RM., 1987. *Reconstruction of the defective cerebellar circuitry in adult Purkinje cell degeneration mutant mice by Purkinje cell replacement through transplantation of solid embryonic implants*. Neuroscience. Jan;20(1):1-22.~~

Spires TL, et al., 2004. *Environmental enrichment rescues protein deficits in a mouse model of Huntington's disease, indicating a possible disease mechanism*. J Neurosci. Mar 3;24(9):2270-6.

Sugawara M., et al., 2007. *Purkinje cell loss in the cerebellar flocculus in patients with ataxia with ocular motor apraxia type 1/early-onset ataxia with ocular motor apraxia and hypoalbuminemia*. European Neurology, vol. 59, no. 1-2, pp. 18–23.

Synofzik M., Ilg W., 2014. *Motor Training in Degenerative Spinocerebellar Disease: Ataxia-Specific Improvements by Intensive Physiotherapy and Exergames*. BioMed Research International, Article ID 583507.

Tamakoshi K., et al., 2014. *Motor skills training promotes motor functional recovery and induces synaptogenesis in the motor cortex and striatum after intracerebral hemorrhage in rats*. Behav Brain Res. 1;260:34-43.

~~Triarhou LC, et al., 1992. *Intraparenchymal grafting of cerebellar cell suspensions to the deep cerebellar nuclei of pcd mutant mice, with particular emphasis on re-establishment of a Purkinje cell cortico-nuclear projection*. Anat Embryol (Berl).;185(5):409-20.~~

Triarhou LC, et al., 1996. *Amelioration of the behavioral phenotype in genetically ataxic mice through bilateral intracerebellar grafting of fetal Purkinje cells*. Cell Transplant. Mar-Apr;5(2):269-77.

Uhlendorf TL, et al., 2011. *Neuroprotective effects of moderate aerobic exercise on the spastic Han–Wistar rat, a model of ataxia*. Br a i n Re s e a r c h 1 3 6 9 2 1 6 – 2 2 2.

Van Kummer BH, Cohen RW. 2015. *Exercise-induced neuroprotection in the spastic Han Wistar rat: the possible role of brain-derived neurotrophic factor*. Biomed Res Int. ;2015:834543.

Vaynman S., et al., 2004. *Hippocampal BDNF mediates the efficacy of exercise on synaptic plasticity and cognition*. Eur J Neurosci 20:2580–2590.

Vazquez-Sanroman D., et al., 2013. *The effects of enriched environment on BDNF expression in the mouse cerebellum depending on the length of exposure*. Behav Brain Res. 15;243:118-28.

Vivar C., et al., 2013. *All about running: synaptic plasticity, growth factors and adult hippocampal neurogenesis*. Curr Top Behav Neurosci. 15:189-210.

Wang DC, et al., 2015. *Recovery of motor coordination after exercise is correlated to enhancement of brain-derived neurotrophic factor in lactational vanadium-exposed rats*. Neurosci Lett. Jul 23;600:232-7.

Wassef M., et al., 1987. *Cerebellar mutations affecting the postnatal survival of Purkinje cells in the mouse disclose a longitudinal pattern of differentially sensitive cells*. Dev Biol. ;124:379–89.

Zhao YG, et al., 2015. *The autophagy gene Wdr45/Wipi4 regulates learning and memory function and axonal homeostasis*. Autophagy.11(6):881-90.

Figure

Click here to download high resolution image

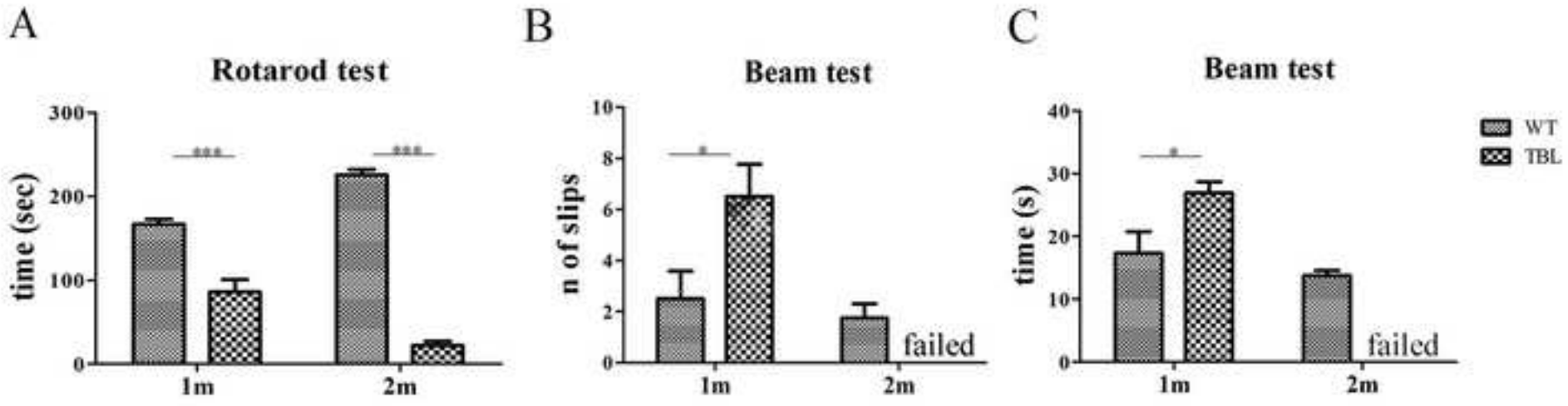

Figure

Click here to download high resolution image

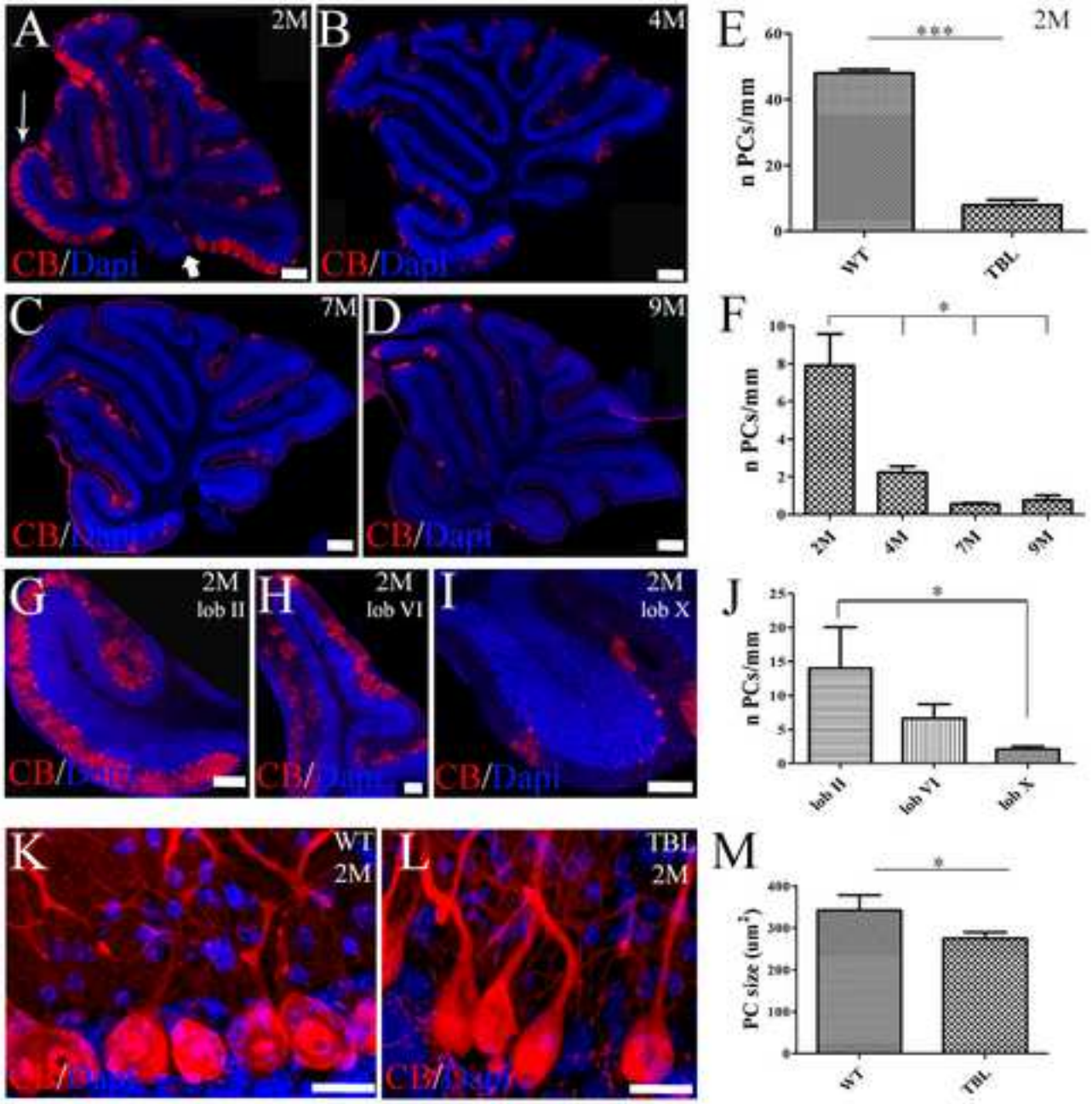

Figure

Click here to download high resolution image

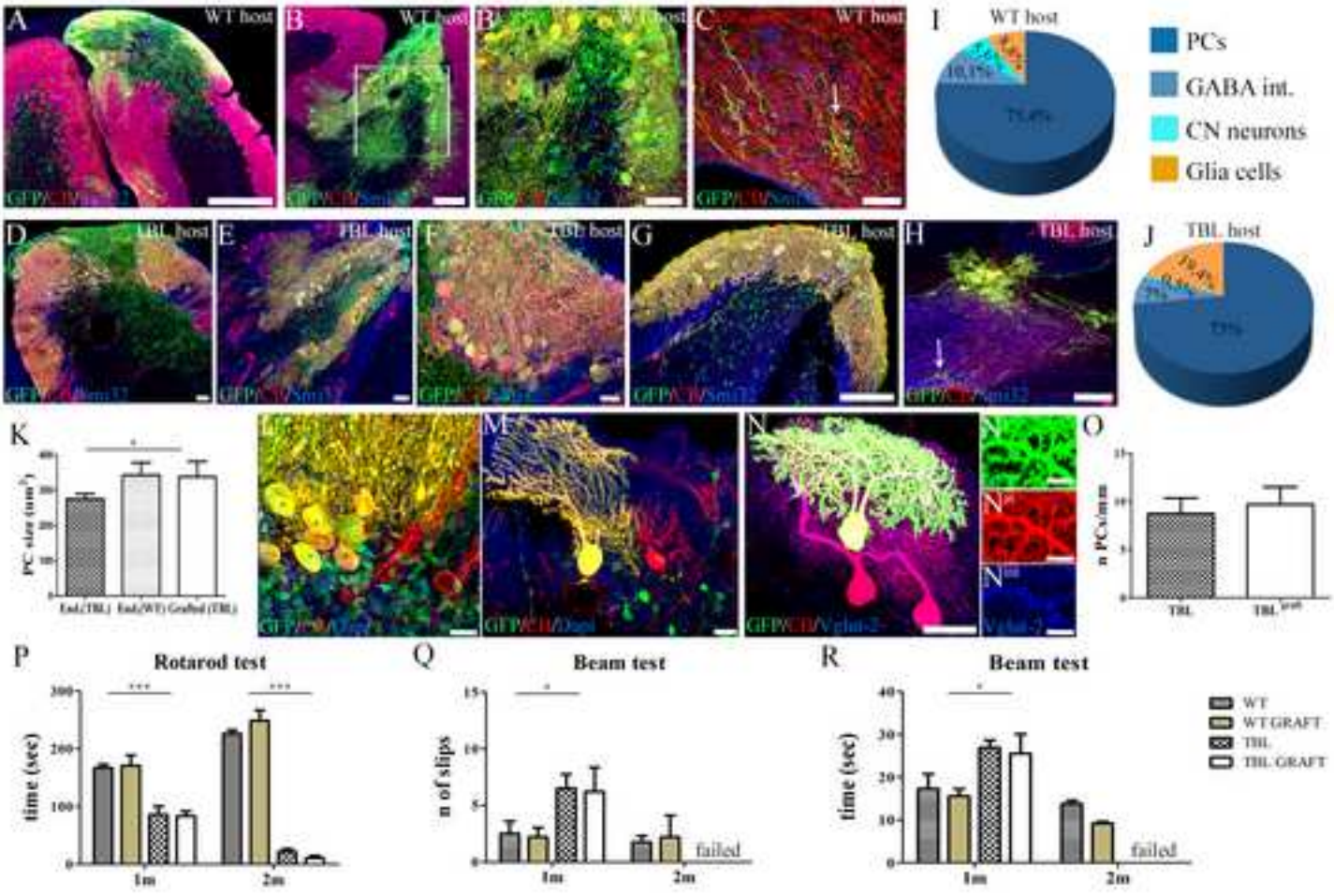

Figure

Click here to download high resolution image

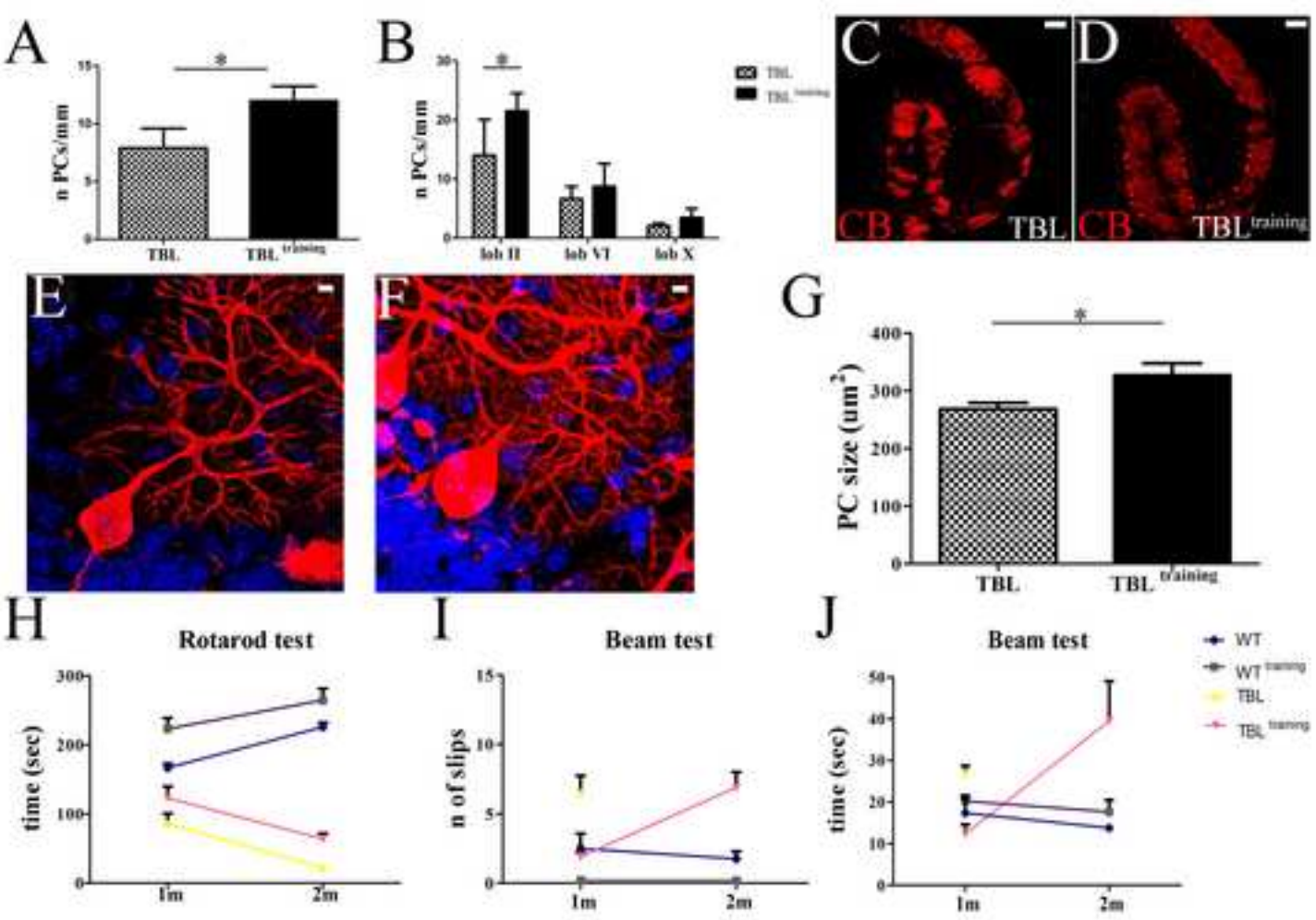

Figure

Click here to download high resolution image

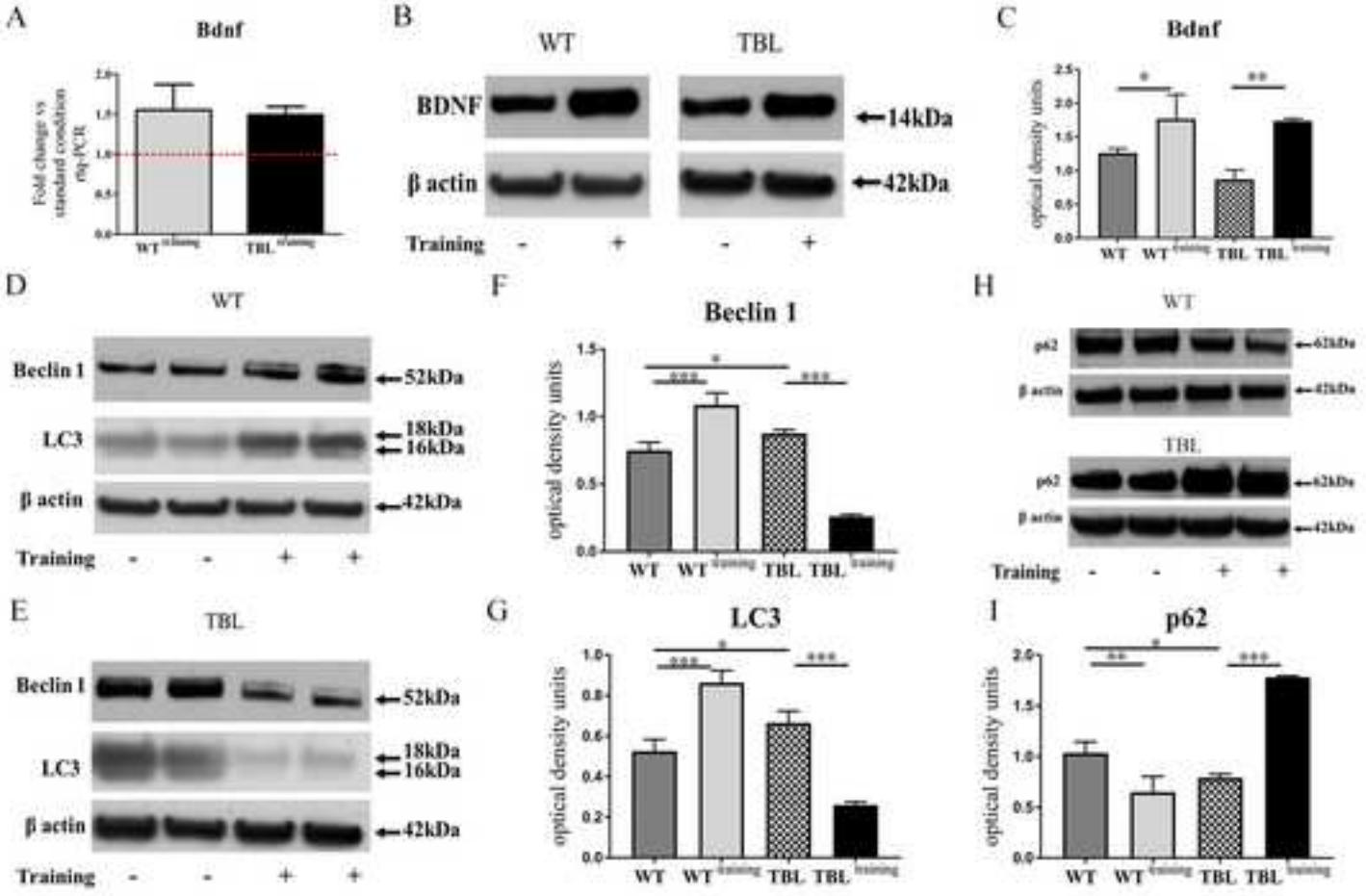

Figure

Click here to download high resolution image

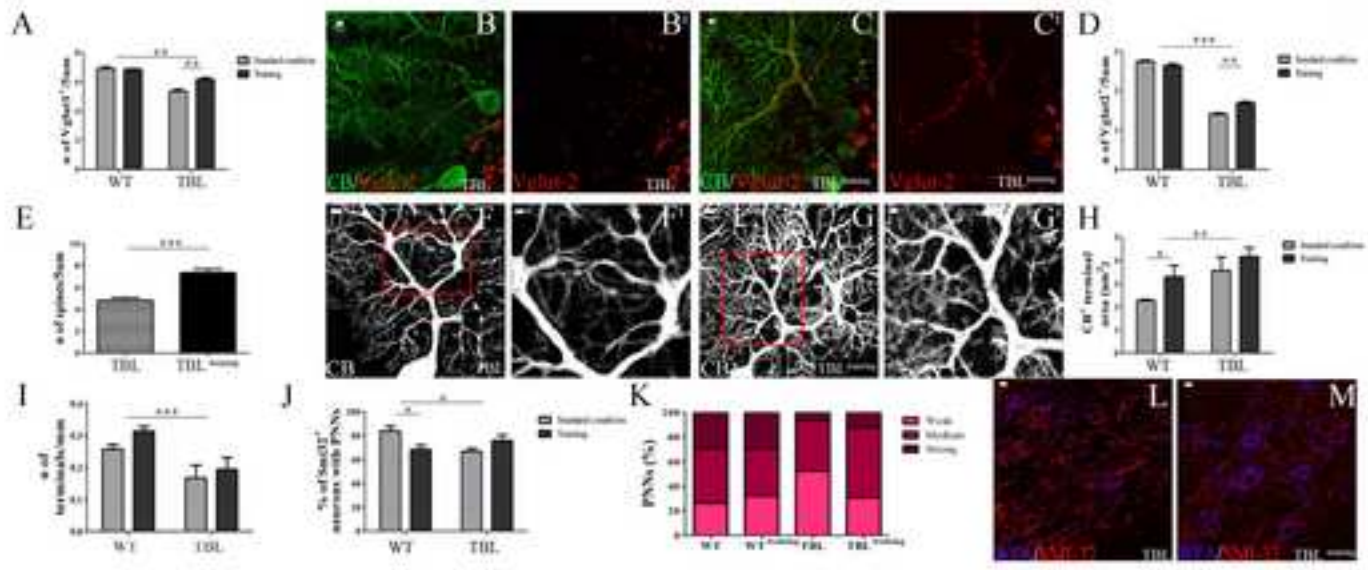

Table

Figure/Table	Applied Test	P value	F value	Post hoc analyses	Post hoc results
Fig 1A	Two-way Anova	P<0.0001	206.13	Bonferroni's Multiple Comparison Test	WT vs tbl, P<0.0001
Fig 1B	Student's t-test	P<0.05	na		
Fig 1C	Student's t-test	P<0.05	na		
Fig 2E	Student's t-test	P<0.0001	na		
Fig 2F	One-way Anova	P<0.05	39.17	Bonferroni's Multiple Comparison Test	2m vs 4/7/9m P<0.05
Fig 2 J	One-way Anova	P<0.05	7.847	Bonferroni's Multiple Comparison Test	Lob II vs Lob X P<0.05
Fig 2M	Student's t-test	P=0.04	na		
Fig 3K	One-way Anova	P=0.036	5.175	Tukey's Multiple Comparison Test	End. (tbl) vs End (WT) P<0.05
Fig 3O	Student's t-test	P=0.7	na		
Fig. 3P	Two-way Anova	Interaction and Genotype: P<0.0001	Interaction =45.83 Genotype =105.75	Bonferroni's Multiple Comparison Test	1/2m WT vs tbl/tbl graft P<0.001 1/2m WT graft vs tbl/tbl graft: P<0.001
Fig. 3Q	Student's t-test wt vs tbl and tbl graft	P=0.028	na		
Fig. 3R	Student's t-test wt vs tbl and tbl graft	P<0.05	na		
Fig. 4A	Student's t-test	P=0.043	na		
Fig.4B	Two-way Anova	Lobule: P<0.0001	Lobule: 83.37	Bonferroni's Multiple Comparison Test	Tbl vs Tbl training: P<0.05
Fig.4G	Student's t-test	P=0.0286	na		
Fig.4H	Two-way Anova	Time and Genotype: P<0.0001	Time =17.46 Genotype =97.06	Bonferroni's Multiple Comparison Test	1m Wt vs WT training: P<0.01 1/2m WT/WT training vs tbl at: P<0.001 1m Wt vs tbl training: P<0.05, 2m P<0.001 1/2m Wt training vs tbl training: P<0.001 2m Tbl vs tbl training: P<0.05.
Fig.4I	One-way Anova 1m One-way Anova 2m	P=0.0017 P=0.0003	8.335 21	Bonferroni's Multiple Comparison Test	1m WT vs tbl: P<0.01; tbl vs tbl training P<0.05 2m WT/wt tr vs tbl tr: P<0.01
Fig.4J	One-way Anova 1m One-way Anova 2m	P=0.0075 P=0.0054	6.221 9.878	Bonferroni's Multiple Comparison Test	1m. WT vs tbl and tbl vs tbl training:P<0.05; 2m wt vs tbl tr: P<0.01; wt tr vs tbl training P<0.05
Fig.5C	One-way Anova	Treatment:P=0.0430 and P=0.0031	13.3	Bonferroni's Multiple Comparison Test	WT vs WT training:P<0.05; tbl vs tbl training:P<0.01
Fig.5 F	One-way Anova	Genotype:P=0.0334 Treatment:P<0.0001	158.3	Bonferroni's Multiple Comparison Test	WT vs tbl:P<0.05; wt vs wt training and tbl vs tbl training:P<0.0001
Fig.5G	One-way Anova	Genotype:P=0.0120 Treatment:P<0.0001	121.6	Bonferroni's Multiple Comparison Test	WT vs tbl:P<0.05; WT vs WT training and tbl vs tbl training:P<0.0001

Fig.5I	One-way Anova	Genotype:P=0.0388 Treatment:P=0.0037 and P<0.0001	61.14	Bonferroni's Multiple Comparison Test	WT vs tbl:P<0.05; WT vs WT training:P<0.01; tbl vs tbl training:P<0.0001
Fig.6A	Two-way Anova	Genotype:P<0.001 Treatment:P=0.0033 Interaction: P<0.0018	Genotype: 188.70 Treatment: 22.21 Interaction: 28.35	Bonferroni's Multiple Comparison Test	WT and WT training vs tbl: P<0.0001; WT and WT training vs tbl training: P<0.01; tbl vs tbl training: P<0.01
Fig.6D	Two-way Anova	Genotype:P<0.0001 Interaction: P<0.0001	Genotype: 929.1 Interaction: 26.95	Bonferroni's Multiple Comparison Test	Wt and WT training vs tbl and tbl training: P<0.001 Tbl vs tbl training: P<0.01
Fig.6E	Student's t-test	P=0.0005	na		
Fig.6H	Two-way Anova	Treatment=P<0.0112 Genotype= P<0.0023	Treatment=10.76 Genotype =19.22	Bonferroni's Multiple Comparison Test	WT vs WT training: P<0.05
Fig.6I	Two-way Anova	Treatment P=0.0413 Genotype P=0.0003	Treatment=5.90 Genotype =37.44	Bonferroni's Multiple Comparison Test	
Fig.6J	Two-way Anova	Genotype:P<0.03 Interaction: P<0.0079	Genotype: 1.7 Interaction: 11.54	Bonferroni's Multiple Comparison Test	Wt vs tbl: P<0.05 WT vs WT training: P<0.05
Fig.6K	Chi-square		na		Wt vs WT training: ns; WT vs tbl:P=0.0005; WT vs tbl training: ns; tbl vs tbl training: P=0.04; WT training vs tbl training: P=0.0275.

Details of performed statistical analyses. Only comparisons leading to P<0.05 are reported.

Supplementary Material

Click here to download Supplementary Material: Supplementary.tif